Novel (super)hard SiCN from crystal chemistry and first principles

Samir Matar, Jean Etourneau, Vladimir Solozhenko

Novel (super)hard SiCN from crystal chemistry and first principles

Samir F. Matar [1,*], Jean Etourneau [2] and Vladimir L. Solozhenko [3]

[1] Lebanese German University (LGU), Sahel Alma, Jounieh, Lebanon
https://orcid.org/0000-0001-5419-358X

[2] University de Bordeaux, ICMCB-CNRS, 33600 Pessac, France
https://orcid.org/0000-0002-9058-9079

[3] LSPM–CNRS, Université Sorbonne Paris Nord, 93430 Villetaneuse, France
https://orcid.org/0000-0002-0881-9761

[*] *Former DR1-CNRS senior researcher at the University of Bordeaux, ICMCB-CNRS, France*
Corresponding author emails: s.matar@lgu.edu.lb and sfm68@hotmail.com

Abstract

The purpose of this work is to predict the existence of novel equiatomic SiCN based on tetragonal C_6 structure (glitter), the elementary building unit being the 1,4 cyclohexadiene molecule comprising both tetrahedral (sp^3) and trigonal (sp^2) carbons. From crystal chemistry rationale the structural transformations of C_6 to SiC_2 and then to SiCN ternary phase were fully relaxed to the ground states using first principles DFT-based calculation. Like early proposed C_6 and SiC_2, SiCN was found bonding and structurally stable from the elastic properties on one hand and dynamically stable from the phonons, on the other hand. The Vickers hardness of SiCN is higher than that of cubic silicon carbide, a conventional superabrasive, whereas hardness of tetragonal SiC_2 is slightly lower. Besides the abrasive properties, the electronic band structure indicates metal-like behavior of SiCN thus suggesting the potential for heat dissipation in operating conditions, oppositely to insulating SiC.

Keywords

Silicon carbonitride; DFT; phonon dispersions; superabrasive; electronic band structure.

Introduction

Whereas SiC is a rather well-studied binary compound that is widely used for various applications [1], ternary compounds of the Si-C-N system are ill-studied. In 1965, equiatomic SiCN was reported as made by SiC crystals grown in nitrogen atmosphere [2]. The stated structure shown in Fig. 1a is a cubic fluorite-like one with face centered Si substructure, and C and N atoms occupying the fluorite F8 cube corners. Later, Chen et al. [3] identified crystalline and amorphous SiCN in the process of thin films growth by microwave CVD; but no crystal structure was reported. The conducted nano-indentation study revealed a hardness value of 30 GPa for the crystalline phase and 22 GPa for the amorphous phase, therefore, the authors' claim that SiCN is a hard material that rivals cubic BN is unjustified. In 1997, Riedel *et al.* [4] claimed the first ternary crystalline solid with $Si_8C_4N_{16}$ stoichiometry built of SiN_4 tetrahedra interconnected via carbon atoms, thus leading to N_3SiN—C—$NSiN_3$-like chains of tetrahedra (blue, Fig. 1c) along vertical *b*-axis, and corner sharing along horizontal planes The latter feature is also characteristic of the novel SiCN proposed herein, with a mixed N-C coordination polyhedron for Si.

In this work, a novel equiatomic SiCN phase is proposed based on crystal chemistry rationale then quantified by *ab initio* calculations within the well-established density functional theory (DFT) [5].

Crystal Chemistry rationale

The chemistry of the silicon with carbon and nitrogen is ruled by several factors involving:

(i) the difference of –Pauling– electronegativities with $\chi(N) = 3.04 > \chi(C) = 2.55 > \chi(Si) = 1.80$ leading to polar Si–C and Si–N ~~polar~~ bonds.

(ii) the larger size of covalent radius: $r_{Si}= 1.14$ Å versus $r_C= 0.76$ Å and $r_N= 0.70$ Å resulting from the atomic configuration exceeding carbon and nitrogen with one more shell, i.e., Si ($1s^2\ 2s^2\ 2p^6\ 3s^2\ 3p^2$) *versus* C ($1s^2\ 2s^2\ 2p^2$) and N ($1s^2\ 2s^2\ 2p^3$) leading to more compressible Si based compounds.

(iii) the tetrahedral coordination (sp^3-like), common to Si, C, and N which also exhibit linear sp and trigonal sp^2 types. However, in rare occurrences, Si=Si (double bonds) and Si≡Si (triple bonds) are known mainly in organic chemistry as in *tetramesityldisilene* [6].

As a case study on the interconnectedness between solid state and molecular chemistry regarding carbon, we have shown recently that the rarely occurring tricarbon C_3 molecule can be a building block of 3D covalent ultra-hard carbon networks, with carbon showing two hybridization types: linear- and tetrahedral-like [7]. Earlier, Bucknum and Hoffman in 1994

[7] conceived a dense hexacarbon tetragonal structure with linear C=C (sp^2) and tetrahedral C(sp^3) based on *1,4-cyclohexadiene.* Such molecule depicted in Fig. 2a is used as an effective hydrogen donor for catalytic hydrogenation reactions. Whereas in butadiene there are alternating double and single bonds between the six carbon atoms (Kekulé formulation) in two resonant formulas, *1,4-cyclohexadiene* shows a localization of two C=C double bonds. The corresponding 3D (D = dimension) structure called 'glitter' [8] i.e., *shining* due to the conductive character of the electronic structure as shown in the bad structure section development of this work (cf. Figure 5). The crystal structure featuring a *C6* hexahedron is shown in Fig. 2b. It consists of two types of carbons labeled C1 (tetrahedral) and trigonal C2, letting express the chemical formula as $C1_2C2_4$.

Later, a silicon dicarbide Si_2C_4 (Fig. 2c) was theoretically proposed based on tetragonal C_6, by replacing tetrahedral C1 by Si leading to *SiC4* tetrahedra connected through the two C2 characterizing the structure [9]. With the objective of identifying SiCN ternary compound in view of the inefficiency of the cubic setup proposed earlier [2], or of cyanide-like SiCN, we come up with the equiatomic stoichiometry through replacing one of the two trigonal carbons (C2) by N leading to *SiC2N2* tetrahedra. The *ad hoc* structure submitted to unconstrained geometry relaxation led to a lowering of the tetragonal space group symmetry to $P4_2mc$ N°105. The ground state equiatomic structure is depicted in Fig. 2d. To the best of our knowledge, no propositions have been made of equiatomic SiCN structure or existence other than the 1965 paper [2].

Computational framework

The search for the ground state structures and their energies such as those devised from crystal chemistry rationale, is a prerequisite to discriminate stable from unstable chemical systems prior to further investigations of the physical properties.

Such a task is best carried within quantum mechanical computations based on the DFT [5]. In present work, our investigations, were carried out using the Vienna Ab initio Simulation Package (VASP) code [10, 11] and the built-in projector augmented wave (PAW) method [11, 12] considering atomic potentials. The DFT exchange-correlation XC effects were considered within the generalized gradient approximation (GGA) [13] found herein to perform like more sophisticated hybrid functional as the GGA-HSE06 [14]. From heavy preliminary calculations, cohesive energies with hybrid functional were found close but slightly larger than the plain GGA results. Such overestimation could lead to validate unstable structures/compositions as the SiCN found unstable also from elastic and dynamic properties in the elaboration of this work.

From the ground state structures the sets of elastic constants C_{ij} were calculated, and the mechanical properties such as hardness and fracture toughness were estimated using contemporary theoretical models. To verify the dynamic stability of the different phases, the phonon dispersion bands were calculated. The approach consists of computing the phonon modes through finite displacements of the atoms off their equilibrium positions to subsequently obtain the forces from the summation over the different configurations. The phonon dispersion curves along the main lines of the tetragonal Brillouin zone (BZ) were obtained using first-principles phonon calculation code "Phonopy" [15]. Finally, the electronic band structures showing small gap insulating to metallic behaviors were assessed.

Results and Discussions

Energies and crystal structures

The structures presented in the introduction were submitted to unconstrained geometry relaxation to obtain the ground state configuration. Energy is the prevailing criterion for a first assessment of the crystal structures.

From the total electronic energies (E_{tot}) the cohesive energies were obtained by deducting the atomic contributions. In view of the different stoichiometries, only the atom averaged cohesive energies can be compared.

Cubic SiCN structure templates

The structure of cubic SiCN (space group *F*-43*m*, N°216) is shown in Fig. 1a resembling fluorite-type is built of face centered Si substructure with C and N occupying cube corners [2]. Replacing N by C to model cubic SiC_2 for the sake of comparison in present work leads to higher symmetry fluorite-type (*Fm*-3*m* N°225) shown in Fig. 1b. Both cubic SiCN and SiC_2 were submitted to unconstrained geometry optimization calculations of the energy. The numerical results of the cohesive energies obtained by subtracting the atomic contributions from the total electronic energy are shown in the first lines of Table 1. They reveal small positive magnitudes leading to doubt the validity of cubic SiCN structure and to search for alternatives.

The ordered structure of orthorhombic equiatomic sodium cyanide NaCN [16] was considered by replacing Na by Si and operating full geometry optimizations. The resulting geometry consisted of a layered structure with square planar *SiC2N2* motifs (Fig. 1d). Such coordination is unusual for Si. The cohesive energy, while being negative, i.e., favored with respect to cubic SiCN, is of a lower magnitude versus the other configurations based of C_6 Glitter as

shown in next paragraph to feature tetrahedral coordinated silicon. Such layered structure hypothesis with square planar *SiC2N2* motifs was subsequently abandoned.

Lastly, the other alkaline cyanides *A*CN (*A* = Li, K, Cs) characterized solely by *A*-N connections were also considered in the preliminary calculations but all led to lower cohesive energies versus square-planar NaCN-type SiCN (Fig. 1c). Such results can be chemically expected since *A*CN cyanides are *A*+ CN-, i.e.,"ionic", whereas SiCN cannot be a cyanide but rather a carbonitride, whence the interest in proposing a stable phase with tetrahedral *SiC2N2* motifs.

Glitter-derived SiCN

The second part of Table 1 shows cohesive chemical systems all larger than the preliminary results at upper part of the table. C_6 which contains both tetrahedral and trigonal carbon types is characterized with $E_{coh.}$/at.= -2.037 eV/at., i.e. less cohesive than diamond made of purely C(sp^3) -cf. [17]. $Si_2C_2N_2$ is cohesive with $E_{coh.}$/at. magnitude smaller but close to that of Si_2C_4. Crystallographically, the replacement of C1 by Si in $C1_2C2_4$ ("glitter" C_6, Fig. 2b) leads to hypothetic silicon dicarbide Si_2C_4 (Fig. 2c) [9] which shows the same tetrahedral stacking as in C_6. Both structures are defined in tetragonal space group $P4_2/mmc$, N° 131 (cf. Tables 1 and 2). Since the two C2 belong to the same Wyckoff site (4*i*), the replacement of one carbon by nitrogen leads to $Si_2C_2N_2$ where Si is tetrahedrally coordinated with trigonal N and C. The initial tetragonal space group $P4_2/mmc$ N° 131 symmetry is lowered and subsequent crystal structure determinations after geometry relaxation led to define the ternary phase in a new space group $P4_2mc$ N°105 (Fig. 2c), i.e., with the loss of a mirror (*m*) symmetry due to the occupation of the fourfold (4*i*) ½, 0, *z* position in Si_2C_4 (Table 2b) by two different atoms, N and C, which are now are in twofold (2c) ½, 0, *z* positions (Table 2c). The trigonal carbon interatomic distances increase from C_6 with d(C2-C2) = 1.34 Å to ~ 1.37 Å in Si_2C_4 due to large Si atom resulting in the increase of *a* and *c* lattice constants. $Si_2C_2N_2$ structure has larger d(C-N) = 1.38 Å while d(Si-C) = 1.82 Å and d(Si-N) = 1.81 Å become close in magnitudes. Note that the tetrahedral angle ∠C-Si-N = 109.76° presents an interesting feature of sp^3-like environment. This is a relevant result in view of the symmetry lowering to tetragonal space group $P4_2mc$ N°105. Consequently, SiCN is likely to exist in a structure with mixed N, C coordination expressed in regular *SiC2N2* tetrahedra connected via C-N along the tetragonal *c*-axis direction. Figure 2e shows a 2×2×1 supercell of SiCN highlighting the *SiC2N2* tetrahedra shown in the same blue color as Si.

Charge density projections

Further illustration of *electronic ↔ crystal-structure* relationship is provided by the charge density projections. Figure 3 shows the charge density yellow volumes in the different panels. In "glitter" C_6 (Fig. 3a) the charge density is expectedly different between tetrahedral C1 with sp^3-like 4-lobes yellow shapes versus trigonal C2 (sp^2-like with linear-like yellow volumes) thus confirming the difference of chemical behavior between carbons belonging to the two crystal sites.

Upon replacing C1 by Si the charge density changes significantly with a transfer from Si to C2. C2-C2 groups show a larger charge envelop versus C2-C2 in C_6 (Fig. 3b). Nevertheless, Si keeps a tetrahedral coordination with C, forming *SiC4* tetrahedra.

The replacement of one C2 by N, leading to $Si_2C_2N_2$ equiatomic compound results in a differentiated charge envelop along the C-N pairs with the largest charge volume around N (Fig. 3c). These results are chemically sound is so far that they go along with the electronegativity trends: $\chi(N) = 3.04 > \chi(C) = 2.55 > \chi(Si) = 1.80$ which coincide with the trends of charge transfers from Si to both C and N, i.e., $\delta(N) = -2.12$, $\delta(C) = -1.72$, and $\delta(Si) = +3.84$.

Mechanical properties

Elastic constants

The elastic constants C_{ij} are needed to derive the mechanical properties. They were determined by performing finite distortions of the lattice and deriving C_{ij} from the strain-stress relationship. Then the bulk *B* and shear *G* moduli are obtained by averaging the single-crystal elastic constants using, here, Voigt's method [18] based on a uniform strain. The calculated sets of elastic constants are given in Table 3. All values are positive, which is the first indication of mechanical stability. Further proofs were obtained from C_{ij} combinations obeying rules related to mechanical stability: C_{ii} (i =1, 3, 4, 6) > 0; $C_{11} > C_{12}$, $C_{11}+C_{33} - 2C_{13} > 0$; and $2C_{11}+ C_{33} + 2C_{12} + 4C_{13} > 0$.

The equations providing the bulk B_V and shear G_V moduli as function of the elastic constants C_{ij} are as follows for the tetragonal system:

$B_{Voigt}^{tetr.} = 1/9\ (2C_{11} + C_{33} + 2C_{12} + 4C_{13})$.

$G_{Voigt}^{tetr.} = 1/15\ (2C_{11} + C_{12} + 2\ C_{33} - 2C_{13} + 6C_{44} + 3C_{66})$.

The calculated C_{ij} are given in Table 3. All values are positive, and their combinations obey the rules pertaining to the mechanical stability. C_6 Glitter characterized by shortest interatomic distances has the highest elastic constants. In Si_2C_4 obtained by the replacement

of C1 by larger Si, the resulting bulk and shear moduli lead to drastically lower C_{ij}, as well as $B_{Voigt}^{tetr.}$ and $G_{Voigt}^{tetr.}$. $B_{Voigt}^{tetr.}$ value agrees with literature [9]. The replacement of carbon by silicon possessing a larger radius and the overall resulting larger volume can explain the larger compressibility of Si_2C_4. Turning to the ternary phase $Si_2C_2N_2$, the calculations of the two moduli $B_{Voigt}^{tetr.}$ and $G_{Voigt}^{tetr.}$ lead to significant increase, explained by the smaller d(Si-C) and d(Si-N) versus d(Si-C) in the dicarbide (Table 2). Such results should be further rationalized with the calculation of the hardness in following section.

Hardness

Vickers hardness (H_V) was predicted using two contemporary theoretical models. The thermodynamic (T) model [19] is based on thermodynamic properties and crystal structure, while Lyakhov-Oganov (LO) approach [20] considers topology of the crystal structure, strength of covalent bonding, degree of ionicity and directionality. The fracture toughness (K_{Ic}) was evaluated using Mazhnik-Oganov model [21] which is the only model that allows such predictions. The results on mechanical properties of the considered phases of the Si-C-N system are presented in Table 4. It is worth noting that hardness and bulk moduli (B_0) calculated in the framework of the thermodynamic model are in perfect agreement with available experimental data [3,22-25]. As follows from our findings, Vickers hardness of $Si_2C_2N_2$ is higher than that of cubic silicon carbide c-SiC (Table 4), a conventional superabrasive, whereas the hardness of tetragonal Si_2C_4 is slightly lower.

Dynamical stabilities from the phonons

Further stability criteria can be obtained from the phonon dispersions. Following the method presented in the 'Computational framework' section, the obtained phonon dispersion curves for C_6, Si_2C_4 and $Si_2C_2N_2$ are shown in Fig. 4. In each panel the bands run along the main lines of the tetragonal Brillouin zone.

Along the vertical direction the frequency ω is given in units of Terahertz (THz). Since no negative energy magnitudes are observed, the three structures can be considered as dynamically stable. There are 3N-3 optical modes at high energy and 3 acoustic modes. The acoustic modes start from zero energy (ω = 0) at the Γ point, center of the Brillouin Zone, up to a few Terahertz. They correspond to the lattice rigid translation modes in the crystal (two transverse and one longitudinal). The remaining bands correspond to optic modes. Remarkably, in C_6 **(**Fig. 4a) the highest bands are at 50 THz, a magnitude higher than in diamond where $\omega_{max.}$ ~40 THz [26] observed with Raman vibration spectroscopy. Such high frequency is assigned to the C2-C2 stretching vibrations. The phonons of Si_2C_4 (Fig. 4b) have similar shape but the highest magnitude is now at ω_{max} ~45 THz. This is concomitant with the

overall smaller elastic constants especially C_{33} and the resulting B and G values as well as the hardness. The phonons dispersions of the equiatomic $Si_2C_2N_2$ show different features versus the two binaries with many flat bands resulting from the unique structure of SiC_2N_2 tetrahedra and the strong C-N interaction.

Electronic band structures

The electronic band structures were calculated within DFT based on the Augmented Spherical Wave ASW method [27]. The crystal input data of Table 1 were used. The band structures are depicted in Figure 5. The energy along the vertical direction is with respect to the Fermi level E_F since all systems are metallic-like with bands crossing E_F; note that Si_2C_4 shows vanishingly small band crossing at E_F. Additional calculations using hybrid XC functional didn't change the metallic character identified for C_6 and SiCN, while bringing little changes to SiC_2 that could be considered as semi-conducting with a very small band gap. However, all three phases are far from the behavior of electronically insulating diamond characterized with a large band gap of 5 eV. The present results on electronic band structures can be approached with those of tricarbon allotropes [7] where two kinds of hybridizations were identified for the carbon sites.

Conclusions

The present work focused on the identification of a viable structure of SiCN equiatomic following a protocol involving crystal chemistry rationalization of structures submitted in a second step to unconstrained geometry optimization with DFT-based quantum mechanical calculations. Among different hypotheses, the most stable structure consists of SiC_2N_2 tetrahedra with a stacking resembling tetragonal "glitter" C_6 and the "glitter"-derived silicon dicarbide. Confirmation of the stabilities for "glitter" C_6, silicon dicarbide and SiCN were inferred from the cohesive energies. The mechanical (elastic properties) and dynamic (phonon dispersions) stabilities have been confirmed. From the quantitative hardness assessments SiCN was found to be (super)hard which makes it a prospective superabrasive. Furthermore, metallic properties of SiCN revealed from the electronic band structure provide the potentiality of evacuating heat during operation (machining, etc.), oppositely to SiC which is an insulator.

Acknowledgements

Computational facilities of LGU are acknowledged.

REFERENCES

1. T. Kimoto, J.A. Cooper. Fundamentals of Silicon Carbide Technology: Growth, Characterization, Devices, and Applications. 2014. John Wiley & Sons : Singapore

[2] T. Kawamura, Silicon carbide crystals grown in nitrogen atmosphere. *Mineralogical Journal (Japan),* 1965, **4**, 333-355.

[3] L.C. Chen, K.H. Chen, S.L. Wei, P.D. Kichambare, J.J. Wu, T.R. Lu, C.T. Kuo. Crystalline SiCN: a hard material rivals to cubic BN. *Thin Solid Films*, 1999, **355-356**, 112-116.

[4] R. Riedel, A. Greiner, G. Miehe, W. Dressler, H. Fuess, J. Bill, F. Aldinger. The first crystalline solids in the ternary Si - C - N system. *Angewandte Chemie (Intl. Edition)*, 1997, **36**, 603-606.

[5] D.S. Scholl, J.A. Steckel. Density Functional Theory. A Practical Introduction (c) 2009 Wiley. ISBN: 13 978-0470373170.

[6] R. West, M.J. Fink, J. Michel. Tetramesityldisilene, a Stable Compound Containing a Silicon-Silicon Double Bond. *Science*, 1981, **214**, 1343-1344.

[7]. S.F. Matar, J. Etourneau, V.L. Solozhenko. First-principles investigations of tricarbon: From the isolated tricarbon C_3 molecule to a novel ultra-hard anisotropic solid. *Carbon Trends*, 2022, **61**, 00132. https://doi.org/10.1016/j.cartre.2021.100132

[8] M. J. Bucknum, R. Hoffmann. A Hypothetical Dense 3,4-Connected Carbon Net and Related B_2C and CN_2 Nets Built from 1,4-Cyclohexadienoid Units. *J. Am. Chem. Soc*. 1994, **116**, 11456-11464.

[9] R.C. Andrew, M. Braun, N. Chetty. A theoretical investigation of the stability of crystalline silicon dicarbide. *Comput. Mater. Sci*. 2012, **55**, 186-191.

[10] G. Kresse, J. Furthmüller, Efficient iterative schemes for ab initio total-energy calculations using a plane-wave basis set. *Phys. Rev. B,* **1996**, 54, 11169.

[11] G. Kresse, J. Joubert, From ultrasoft pseudopotentials to the projector augmented wave. *Phys. Rev. B,* 1999, **59**, 1758-1775

[12] P.E. Blöchl, Projector augmented wave method. *Phys. Rev. B* 1994, **50**, 17953-17979.

[13] J. Perdew, K. Burke, M. Ernzerhof, The Generalized Gradient Approximation made simple. Phys. Rev. Lett. 1996, **77**, 3865-3868.

[14] J. Heyd, G.E. Scuseria and M. Ernzerhof, Hybrid functionals based on a screened Coulomb potential. *J. Chem. Phys.,* 2006, **124**, 219906.

[15] A. Togo, I. Tanaka, First principles phonon calculations in materials science. *Scr. Mater*. **108,** 2015, 1-5.

[16] D. Fontaine, Structure du cyanure de sodium en phase ordonnée. *Comptes Rendus des Séances de l'Académie des Sciences. Série B.* **281**, 1975, 443-444.

[17] S.F. Matar, V.L. Solozhenko. Novel ultra-hard hexacarbon allotropes from first principles. ChemRxiv 2022. Theoretical and Computational Chemistry. DOI 10.26434/chemrxiv-2022-x4p38. Under revision with Solid State Sciences (Feb. 2022).

[18] W. Voigt, Über die Beziehung zwischen den beiden Elasticitätsconstanten isotroper Körper. *Annal. Phys*. **274**, 1889, 573-587.

[19] V.A. Mukhanov, O.O. Kurakevych, V.L. Solozhenko, The interrelation between hardness and compressibility of substances and their structure and thermodynamic properties. *J. Superhard Mater*., 2008, **30**, 368-378.

[20] A.O. Lyakhov, A.R. Oganov, Evolutionary search for superhard materials: Methodology and applications to forms of carbon and TiO_2. *Phys. Rev. B,* 2011, **84**, 092103.

[21] E. Mazhnik, A.R. Oganov, A model of hardness and fracture toughness of solids. *J. Appl. Phys.*, 2019, **126**, 125109.

[22] L.J. Vandeperre, F.Giuliani, S.J. Lloyd, W.J. Clegg. The hardness of silicon and germanium. *Acta Mater*., 2007, **55**, 6307-6315.

[23] S.N. Vaidya, G.C. Kennedy. Compressibility of 22 elemental solids to 45 KB. *J. Phys. Chem. Solids*, **33** , 1972, 1377-1389.

[24] M. Baloga, P. Šajgalík, M. Hnatko, Z. Lenčéš, F. Monteverde, J. Kečkéš, J.-L. Huang. Nano- versus macro-hardness of liquid phase sintered SiC. *J. Eur. Ceram. Soc.,* 2005, **25,** 529-534.

[25] K. Strössner, M. Cardona, W.J. Choyke. High pressure X-ray investigations on 3C-SiC. *Solid State Commun*., 1987, **63**, 113-114.

[26] R.S. Krishnan. Raman spectrum of diamond*. Nature*, **155** , 1945, 171.

[27] V. Eyert. Basic notions and applications of the augmented spherical wave method. *Int. J. Quantum Chem.*, **77** , 2000, 1007-1031.

Table 1 Total energies (E_{tot}) and atom averaged cohesive energies (E_{coh}/atom.) of different phases considered in the present work.

Phase	Space Group	Number	$E_{Tot.}$ (eV)	$E_{Coh.}$/at. (eV)
c-$Si_4C_4N_4$ [2]	*F*-43*m*	N°216	-73.38	+0.054
c-Si_4C_8*	*Fm*-3*m*	N°225	-72.32	+0.340
o-$Si_2C_2N_2$[15]	*Pmmn*	N°59	-44.12	-1.210
C_6	$P4_2/mmc$	N°131	-51.82	-2.037
Si_2C_4 (SiC_2)	$P4_2/mmc$	N°131	-45.21	-1.458
$Si_2C_2N_2$(SiCN)	$P4_2mc$	N°105	-45.37	-1.418

* Structure based on Ref. 2

Atomic energies in eV: Si (-5.03); C (-6.6); N (-6.8).

Table 2 Calculated crystal structures parameters.

a) Glitter C_6, space group $P4_2/mmc$ (N° 131). (Fig. 2b).

a = 2.589 Å; c = 5.979 Å.

Atom	Wyckoff	x, y, z
C1	2*b*	½, ½, ¼
C2	4*c*	½, 0, 0.112

d(C2-C2) = 1.34 Å; d(C1-C2) = 1.54 Å.

∠C2-C1-C2 = 106.795°, ∠C1-C2-C2 = 122.517°

b) Si_2C_4 (SiC_2) space group $P4_2/mmc$ (N° 131). (Fig. 2c).

a = 3.170 Å; c = 6.878 Å.

Atom	Wyckoff	x, y, z
Si	2*f*	½, ½, ¼
C	4*i*	½, 0, 0.099

d(C-C) = 1.37 Å; d(Si-C) = 1.89 Å.
∠C-Si-C =113.32°
∠C-C-Si =123.19°

c) $Si_2C_2N_2$ (SiCN) space group $P4_2mc$ (N° 105). (Fig. 2d).

a = 2.9492 Å; c = 6.978 Å.

Atom	Wyckoff	x, y, z
Si	2*b*	½, ½, 0.2507
C	2*c*	½, 0, 0.0986
N	2*c*	½, 0, 0.9007

d(C-N) = 1.38 Å; d(Si-C) = 1.82 Å; d(Si-N)= 1.81 Å.
∠C-Si-N =109.76°

Table 3 Calculated elastic constants and resulting bulk (B_V) and shear (G_V) moduli (in GPa).

	C_{11}	C_{12}	C_{13}	C_{33}	C_{44}	C_{66}	B_V	G_V
C_6	715	45	95	1172	69	71	340	296
Si_2C_4 (SiC_2)	342	5	103	523	36		181*	122
$Si_2C_2N_2$ (SiCN)	429	5	135	718	4	115	236	155

* In agreement with Ref. 9 results.

Table 4 Mechanical properties of some phases of the Si–C–N system: Vickers hardness (H_V), bulk modulus (B), shear modulus (G), Young's modulus (E), Poisson's ratio (ν) and fracture toughness (K_{Ic}).

Phase (space group)	H_V			B			G_V	E ‡	ν ‡	K_{Ic} §
	T*	LO†	exp.	B_0*	B_V	exp.				
	GPa									MPa·m$^{1/2}$
c-Si (227)	12	14	13 [22]	102	90	101 [23]	48	122	0.27	0.7
C_6 (131)	83	75	—	376	340	—	296	688	0.163	5.7
c-SiC (216)	34	30	33 [24]	236	216	248 [25]	126	316	0.26	2.5
Si_2C_4 (131)	31	32	—	183	181	—	122	299	0.225	2.1
c-SiCN (216)	30	41	30 [3]	335	—	—	—	—	—	—
$Si_2C_2N_2$ (105)	38	35	—	228	236	—	155	381	0.231	3.0

* Thermodynamic model [19]

† Lyakhov-Oganov model [20]

‡ E and ν values calculated using isotropic approximation

§ Mazhnik-Oganov model [21]

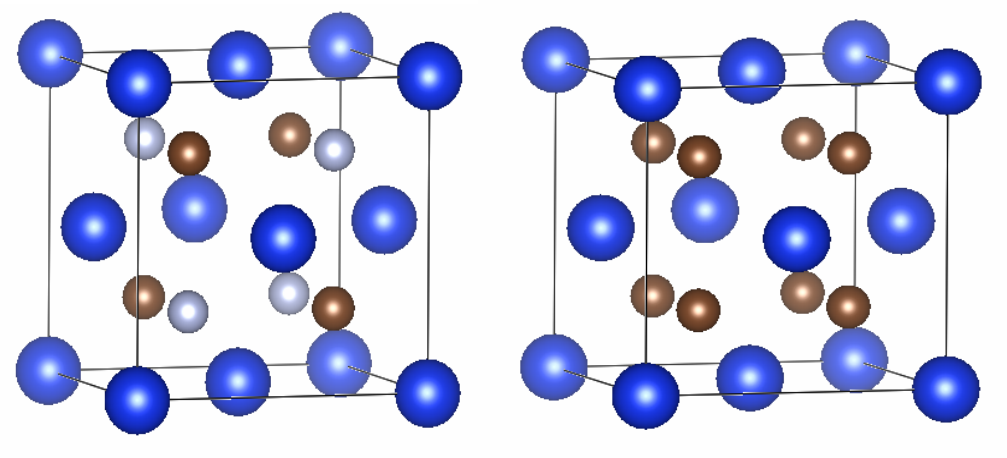

(a) $Si_4C_4N_4$ (b) Si_4C_8

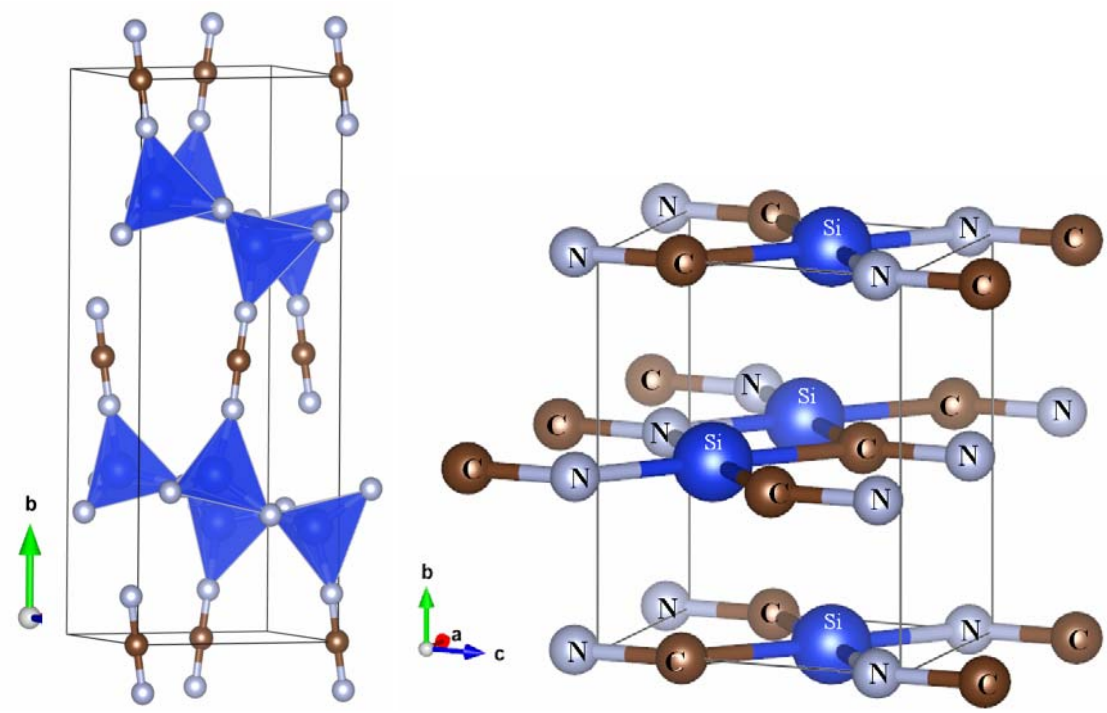

(c) $Si_8C_4N_{16}$ (d) SiCN

Figure 1. Si-C-N ternary structures within preliminary assessments. a) Cubic fluorite-like equiatomic c-$Si_4C_4N_4$ [2], and b) Si_4C_8 derived from cubic $Si_4C_4N_4$; c) $Si_8C_4N_{16}$ [4] showing *SiN4* tetrahedra in blue color, d) optimized SiCN derived from orthorhombic NaCN [15]. Blue, brown, and grey spheres correspond to Si, C and N atoms, respectively.

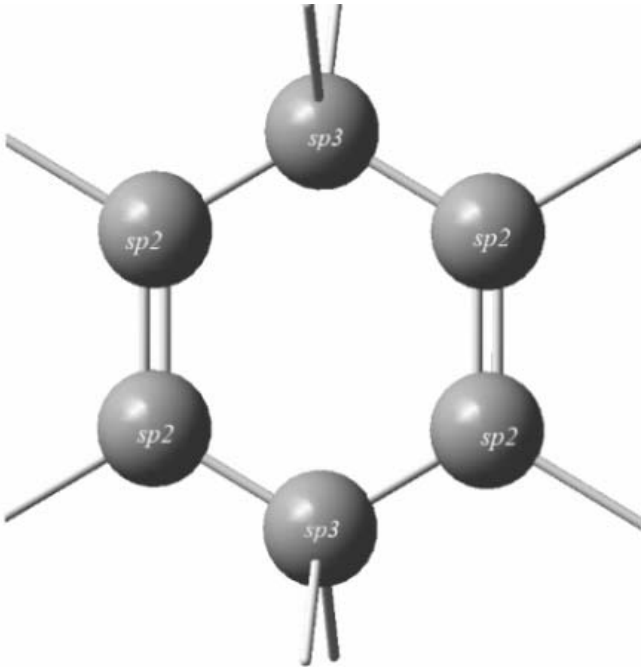

(a)

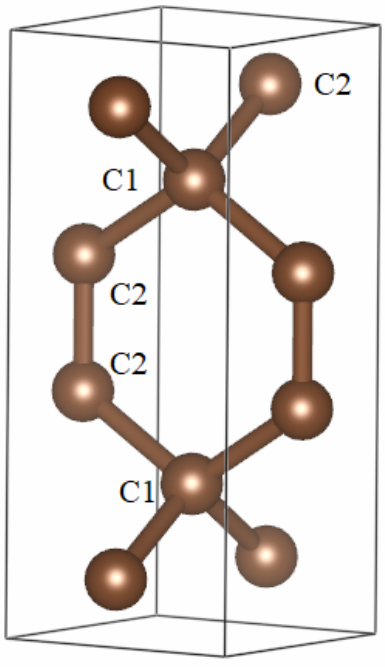

(b)

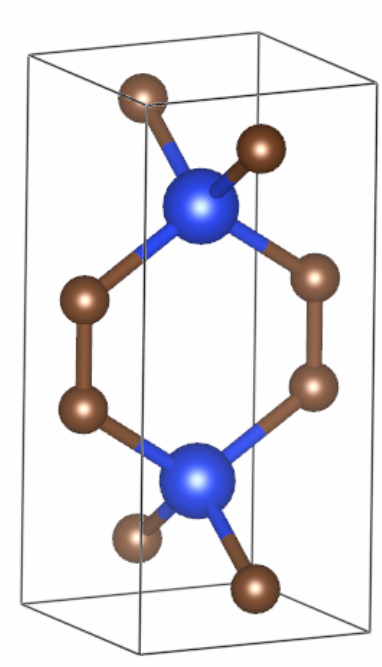

(c)

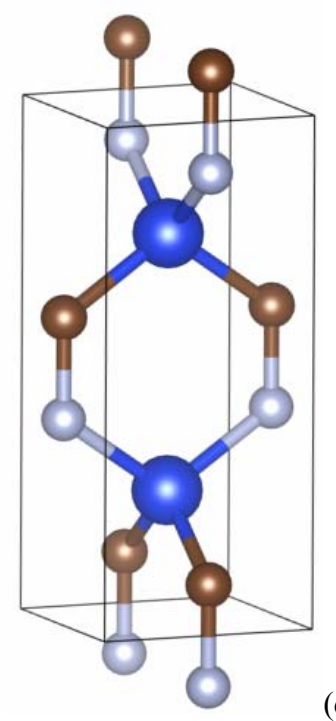

(d)

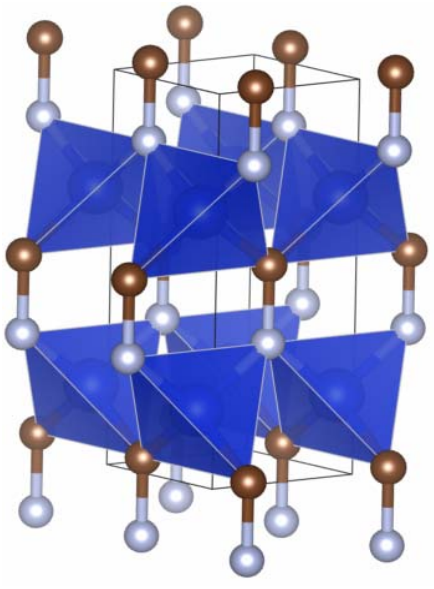

(e)

Figure 2. Sketches of the different structures: (a) 1,4-cyclohexadiene isolated molecule highlighting sp^3 and sp^2 carbons; (b) tetragonal C_6; (c) tetragonal Si_2C_4 (SiC_2); (d) tetragonal equiatomic $Si_2C_2N_2$ (SiCN); (e) 2×2×1 supercell of SiCN highlighting the *SiC2N2* tetrahedra. Blue, brown, and grey spheres correspond to Si, C and N atoms, respectively.

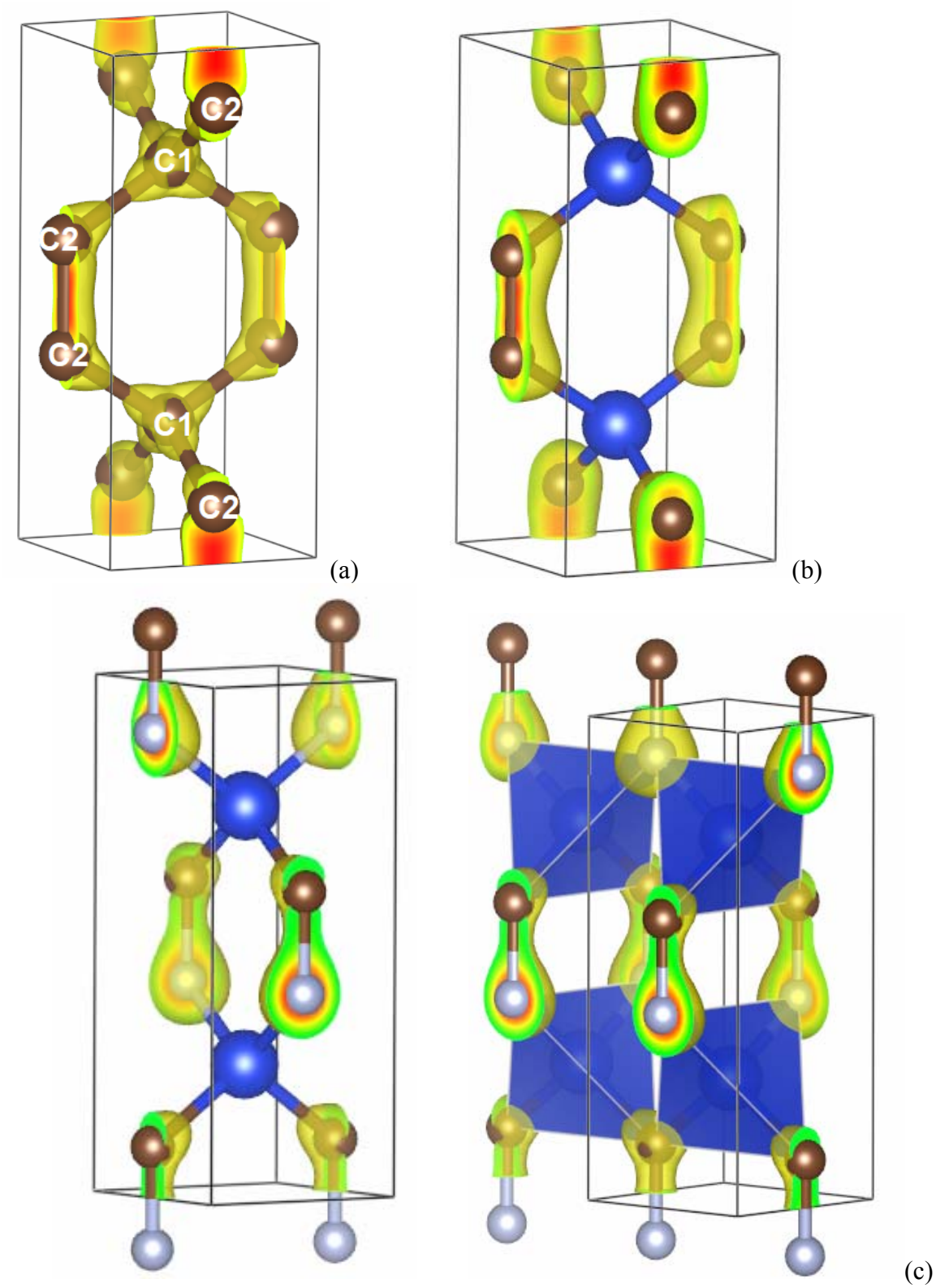

Figure 3. Charge density projections. (a) tetragonal C_6; (b) tetragonal Si_2C_4 (SiC_2); (c) tetragonal equiatomic $Si_2C_2N_2$ (SiCN); with highlighting of blue *SiC2N2* tetrahedra. Blue, brown and grey spheres correspond to Si, C and N respectively.

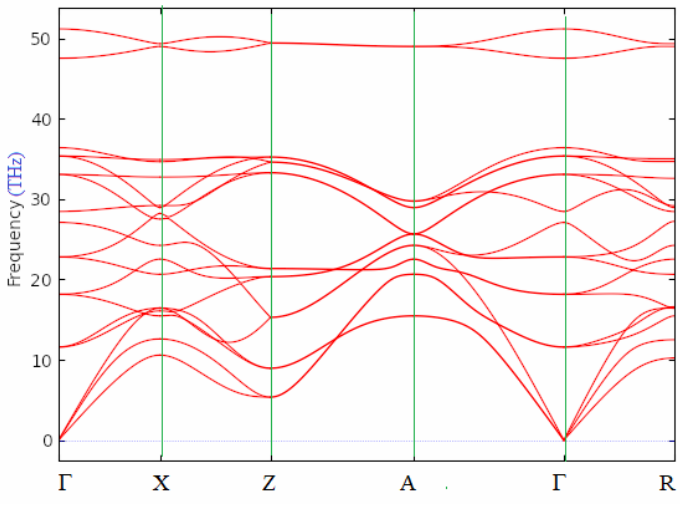

(a)

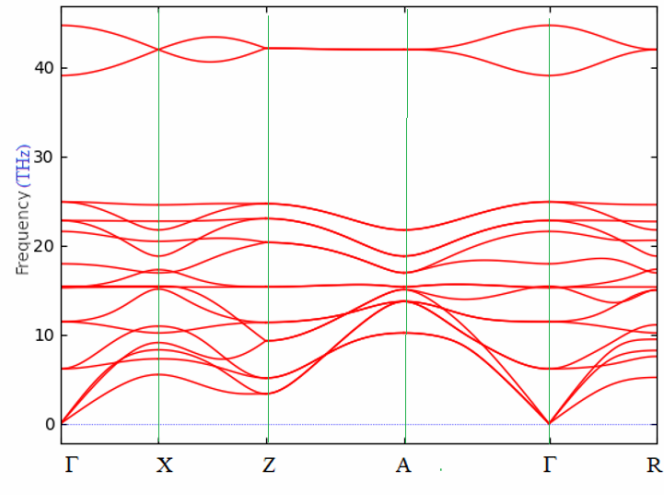

(b)

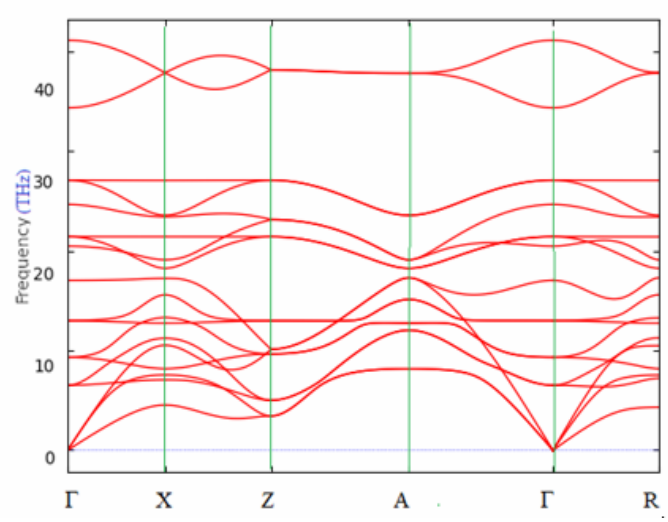

(c)

Figure 4. Phonon dispersions along directions of the tetragonal Brillouin zone. (a) «glitter» C_6; (b) «glitter»-based Si_2C_4 (SiC_2); (c) $Si_2C_2N_2$ (SiCN).

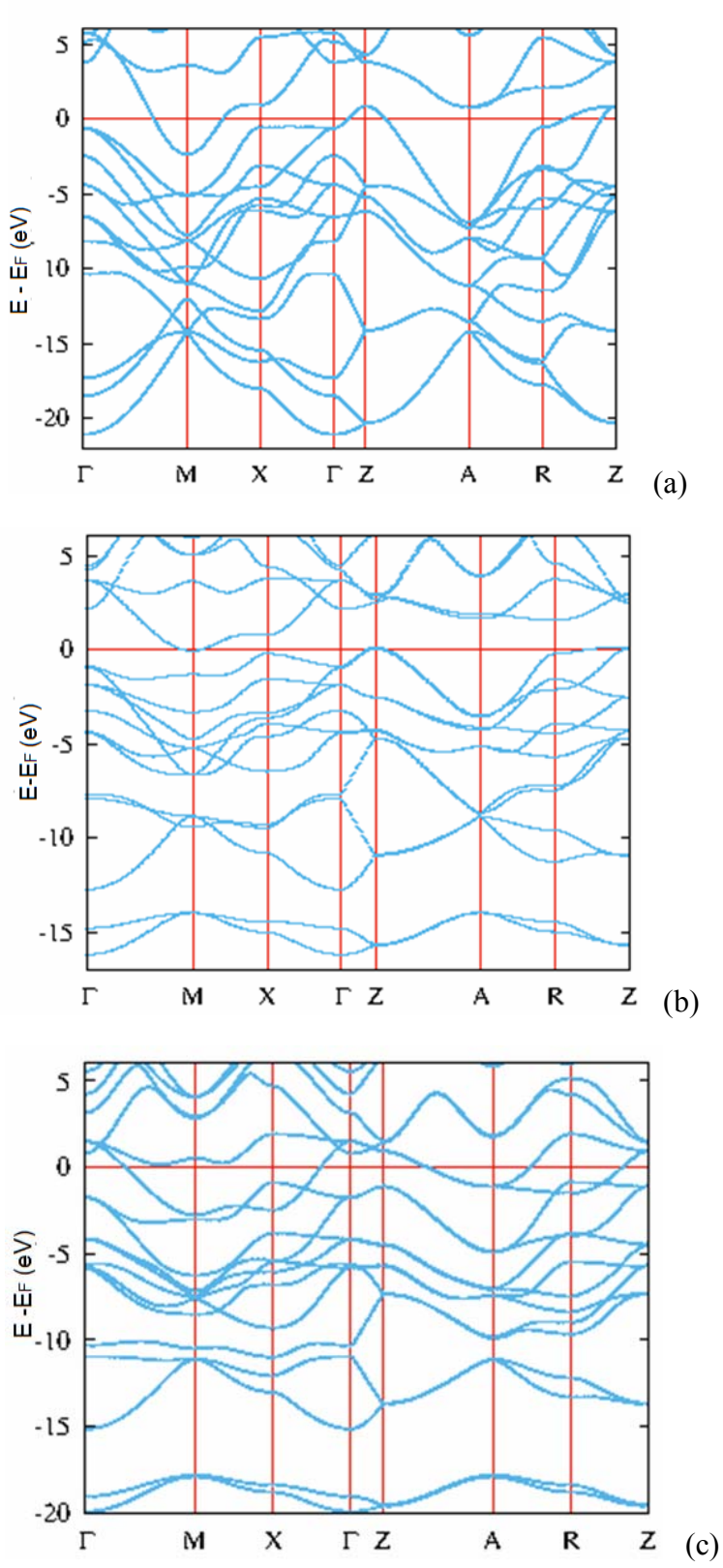

Figure 5 Electronic band structures along main directions of the tetragonal Brillouin zone: (a) "glitter" C_6; (b) "glitter"-based Si_2C_4 (SiC_2); (c) $Si_2C_2N_2$ (SiCN).